ELSEVIER

Journal of Hazardous Materials B114 (2004) 191–197

Journal of Hazardous Materials

www.elsevier.com/locate/jhazmat

Photodegradation of polychlorinated dibenzo-*p*-dioxins: comparison of photocatalysts

Chung-Hsin Wu[a,*], Guo-Ping Chang-Chien[b], Wei-Shan Lee[b]

[a] *Department of Environmental Engineering and Health, Yuanpei University of Science and Technology, 306 Yuanpei Street, Hsinchu City, Taiwan*

[b] *Department of Chemical Engineering, Cheng-Shiu University of Technology, Kaohsiung 833, Taiwan*

Received 18 May 2004; received in revised form 13 August 2004; accepted 18 August 2004
Available online 29 September 2004

Abstract

1,2,3,6,7,8-hexachlorodibenzo-*p*-dioxin (1,2,3,6,7,8-HxCDD) and octachlorodibenzo-*p*-dioxin (OCDD) were photocatalytically degraded using immobilized TiO_2, ZnO and SnO_2 films under ultraviolet (UV) with the wavelength between 300 and 450 nm. The specific surface areas of TiO_2, ZnO and SnO_2 powders were calculated as 54.2, 4.6 and 4.8 m^2/g, and the band gap energies were determined to be 3.17, 2.92 and 4.13 eV, respectively. The light source used had wavelengths between 300 and 450 nm, and the main wavelength was approximately 365 nm; hence, the smaller quantum efficiency of SnO_2 with wider band gap due to poor utilization of the UV light was expected. X-ray diffraction (XRD) revealed that sintered photocatalysts at 400 °C did not alter their characteristics. The first-order rate constants of OCDD in UV/TiO_2, UV/ZnO and UV/SnO_2 were 5.30, 0.74 and 0.28 h^{-1}, respectively; those of 1,2,3,6,7,8-HxCDD in UV/ZnO and UV/SnO_2 were 3.28 and 3.19 h^{-1}, respectively. As expected, photodegradation rates declined as the number of chlorine atoms increased. Due to the low dosage (50 ng) of target compounds used, the amounts of Cl^- and total organic carbon were too small for quantification. No 2,3,7,8-substituted congeners was identified during the photodegradation, and the UV/photocatalyst treatment might offer an effective treatment for PCDDs.

Keywords: Photodegradation; Photocatalyst; TiO_2; ZnO; SnO_2; 1,2,3,6,7,8-HxCDD; OCDD

1. Introduction

Polychlorinated dibenzo-*p*-dioxins (PCDDs) and polychlorinated dibenzofurans (PCDFs) are considered to be persistent in the environment, with little or no degradation [1]. The average half-lives of tetrachlorodibenzo-*p*-dioxin, 1,2,3,7,8-pentachlorodibenzo-*p*-dioxin (1,2,3,7,8-PeCDD), 1,2,3,4,7,8-hexachlorodibenzo-*p*-dioxin (1,2,3,4,7,8-HxCDD), 1,2,3,4,6,7,8-heptachlorodibenzo-*p*-dioxin (1,2,3,4,6,7,8-HpCDD) and OCDD in adult humans are approximately 2840 days, 12.6, 26–45, 80–102 and 112–132 years, respectively [2]. Most PCDD/Fs are formed during municipal waste incinerations. The presence of PCDD/Fs is a potential health risk to humans but only the 2,3,7,8-substituted congeners are toxicologically important. Levels of PCDD/Fs in ambient air and soil near a municipal solid waste incinerator range from 0.058 to 0.127 pg TEQ/m^3 and from 0.524 to 5.02 pg TEQ/g, respectively [3]. The emission concentration of municipal solid waste incinerator at the stack ranged between 0.026 and 4.548 ng TEQ/m^3 [4]. Additionally, the carcinogenic risks of incinerator-emitted dioxin ranged from 1.4×10^{-8} to 7.1×10^{-5} [5]. The 75 PCDDs and 135 PCDFs all differ in the number and position of the chlorine element. More substituted-chloro dioxins generally correspond to a lower vapor pressure, lower solubility and higher half-life [2,6]. These compounds all have high octanol–water coefficients and consequently partition strongly in soil/sediment systems [7].

* Corresponding author. Tel.: +886 5 533 4958; fax: +886 5 5334958.
E-mail address: chwu@mail.yust.edu.tw (C.-H. Wu).

0304-3894/$ – see front matter © 2004 Elsevier B.V. All rights reserved.
doi:10.1016/j.jhazmat.2004.08.008

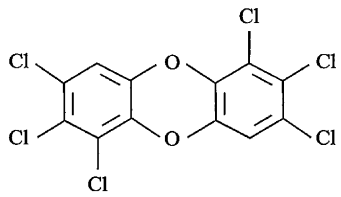

(a) 1,2,3,6,7,8- HxCDD

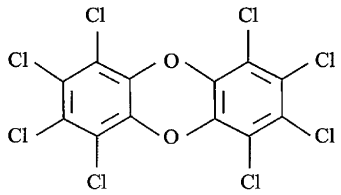

(b) OCDD

Fig. 1. Structural formulas of 1,2,3,6,7,8-HxCDD and OCDD.

In Taiwan, incineration is becoming a dominant method of treating municipal solid waste (MSW). Various methods have been used to reduce the dioxin emission from MSW incinerations; they either inhibit the formation of dioxins or remove them from gas streams. Activated carbon injection technology can effectively reduce the concentration of dioxins in flue gas. However, the practice has the disadvantage of disposal of spent carbon. One approach is to extract dioxins from the spent carbon and then identify an effective method to degrade dioxins. Several methods have been considered in developing an efficient approach for destroying PCDD/Fs, including catalytic destruction [8], photolysis [9,10], photocatalysis [11] and ozonolysis [12]. Those studies essentially address the dechlorinated products that associated the degradation of different PCDD/Fs, with and without the use of photocatalysts. Almost all studies of the photodegradation of PCDD/Fs use catalytic particles suspended in solution with a few exceptions, e.g., Choi et al. [11] and Muto et al. [13] use immobilized TiO_2 film. The advantage of using fixed catalysts is apparent, since the system can prevent: (i) the decline in the availability of light due to the absorption of UV light by particles; (ii) the difficulty in recycling the photocatalyst [14]; and (iii) the difficulty in filtering and separating photocatalyst particles from decontaminated water. Consequently, this study is undertaken to evaluate dioxin degradation in a fixed catalyst system. The target dioxin compounds selected are 1,2,3,6,7,8-HxCDD and OCDD (Fig. 1). OCDD is the most common compound of seventeen 2,3,7,8-subsituted chlorine PCDD/Fs, representing approximately 35% of the total PCDD/Fs concentration in Taiwan [15]. Also, 1,2,3,6,7,8-HxCDD represents a higher-chlorinated congener of PCDD/Fs and to our best knowledge there has been no study using photocatalysts to degrade HxCDD. The present study utilizes photocatalytic films immobilized on quartz to degrade target compounds, since TiO_2 immobilized on quartz exhibited stronger photocatalytic activity than TiO_2 immobilized on stainless steel or glass [16]. Several important characteristics of photocatalytic powders and immobilized films were quantified. For efficiency comparison, three catalysts, TiO_2, ZnO and SnO_2, were used.

2. Materials and methods

2.1. Materials

The target compounds, 1,2,3,6,7,8-HxCDD and OCDD were purchased from Wellington Laboratories (concentration in nonane at 50 μg/ml) and used as obtained. The labeled compounds, [^{13}C]-2,3,7,8-TCDF, [^{13}C]-1, 2,3,7,8-PeCDF, [^{13}C]-2,3,4,7,8-PeCDF, [^{13}C]-1,2,3,4,7,8-HxCDF, [^{13}C]-1,2,3,6,7,8-HxCDF, [^{13}C]-2,3,4,6,7,8-HxCDF, [^{13}C]-1,2,3,7,8,9-HxCDF, [^{13}C]-1,2,3,4,6,7,8-HpCDF, [^{13}C]-1,2,3,4,7,8,9-HpCDF, [^{13}C]-2,3,7,8-TCDD, [^{13}C]-1,2,3,7,8-PeCDD, [^{13}C]-1,2,3,4,7,8-HxCDD, [^{13}C]-1,2,3,6,7,8-HxCDD, [^{13}C]-1,2,3,4,6,7,8-HpCDD, and [^{13}C]-OCDD, were also purchased from Wellington Laboratories (Canada). The TiO_2 used from Degussa (P-25) (Germany), ZnO was purchased from Fluka (Switzerland), and SnO_2 from Riedel-de Haen (Germany).

2.2. Characteristics of photocatalysts

Specific surface areas of photocatalysts were measured using the BET method with Micromeritics ASAP2010 device. The UV–vis spectrum results were used to calculate the semiconductor band gap energy. Moreover, UV–vis spectroscopy was used to profile the absorbance spectrum of the semiconductors from wavelengths 190 to 1000 nm at 500 nm/min with a GBR Cintar 20. Furthermore, the energy of the band gap was calculated by exprapolating a straight line to the abscissa axis. The band gap energies of photocatalysts were determined by substituting the critical wavelengths of photocatalysts into the Planck equation ($E = h\nu$). The crystallinity of the photocatalytic powders and the immobilized films was elucidated by the XRD using Scintag X1. The accelerating voltage and the applied current were 30 kV and 20 mA, respectively. The XRD patterns were recorded for 2θ between 20° and 80° and the scanning speed was 5°/min.

2.3. Photolytic experiments

A TiO_2 film was coated on the quartz plate (20 mm × 20 mm) by dipping the plate into a 5 wt.% TiO_2 suspension and pulling it upward manually. The suspension of catalysts was prepared via stirring for 30 min. Before it was dipped, the quartz surface was first treated using 1% HCl, washed with distilled water and dried at 100 °C. The film was then dried in air, and heat-treated in an atmosphere at 400 °C for 30 min [11]. Subsequent XRD observations revealed that sintering at 400 °C did not alter the crystallinity of photocatalysts. This 400 °C-sintering process was performed five times consec-

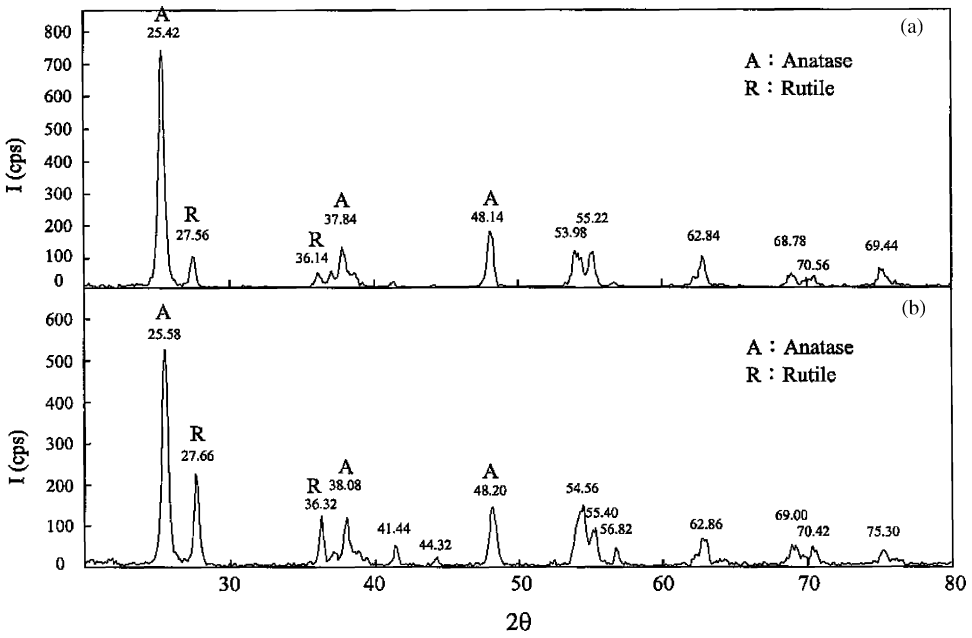

Fig. 2. X-ray diffraction diagram of TiO_2 (a) powder, (b) immobilized film.

utively to increase the total thickness of the film [11,17]. The substrate was also coated with ZnO or SnO_2 films using the same procedure. In the photodegradation experiments, 1 μl aliquot of the target compound (at a concentration in nonane of 50 μg/ml) was loaded on the catalyst coated quartz plates, and the nonane was evaporated in air and the plate was then exposed to UV light. The UV light source was a 400 W medium-pressure Hg lamp (HPA-400), with a spectrum mainly between 300 and 450 nm. Light intensity of the UV light was 6.33 mW/cm^2. The lamp was situated 40 cm from the photocatalysts and the infrared light was not removed by a filter. The air humidity was not specially controlled and was monitored it in the range 70–85% and the temperature of the photocatalysts was 35 °C for all the photocatalytic experiments.

2.4. Analysis of PCDD/Fs

For the extraction of dioxin compounds from the quartz plates, the plates were first treated using 10 ml methanol, and the extracts were spiked with 20 μl of labeled PCDD/F standard [18]. The treated samples were further chromatographically purified using a silica gel column (70–130 mesh, Acme's) with 20 ml of hexane. Extracted PCDD/Fs were then analyzed in the Super Micro Mass Research and Technology Center of Cheng-Shiu University of Technology, using a gas chromatograph/high-resolution mass spectrometer (GC/HRMS). The GC (Hewlett Packard 6890) includes a 60 m length of a DB-5MS capillary column (F&W Scientific, USA), with film thickness 0.25 μm and the column internal diameter 0.25 mm. The oven temperature program was set as follows: 150 °C held for 4 min, then gradually increased to 310 °C and finally held for 5 min at 310 °C. The carrier gas was helium at a flow rate of 1.2 ml/min. The HRMS (Micromass Autospec Ultima, UK) uses a positive electron ionization detector. The analyzer mode for selected ion recording had a resolution of 10,000 (10% valley definition). The electron energy was 35 eV, and the source temperature was 250 °C.

3. Results and discussion

3.1. Characteristics of photocatalysts

Fig. 2 presents the XRD diagrams of TiO_2 powders and the immobilized photocatalyst film, respectively. For practical purpose, the pattern for both powders and immobilized films is essentially the same for all three catalysts (ZnO and SnO_2 are not shown here). The sintering temperature of 400 °C used for immobilization preparation apparently did not alter the catalyst crystallization. The 2θ peaks at 25.4°, 37.8°, and 48.1°, elucidate the typical structure of anatase-type TiO_2, and those 27.6° and 36.1° reveal rutile-type TiO_2 (Fig. 2). The distribution between these two phases is affected by temperature, and 400 °C appears to provide more active anatase phase [17]. However, the relative intensity of anatase-type TiO_2 slightly decreased after 400 °C sintering in this study. ZnO exhibits a hexagonal zincite type structure and the 2θ peaks were 32.2°, 34.8°, 36.6°, 47.9° and 57.0°. SnO_2 crystallizes in a tetragonal cassiterite phase with 2θ peaks at 26.8°, 34.1°, 38.2° and 52.0°.

The crystallite size can be determined from the broadening of the diffraction peak, by applying the Scherrer equation, or $d = 0.89\lambda/\beta \cos\theta$, where d represents the crystal size of the photocatalyst; λ is the X-ray wavelength; β is the full width

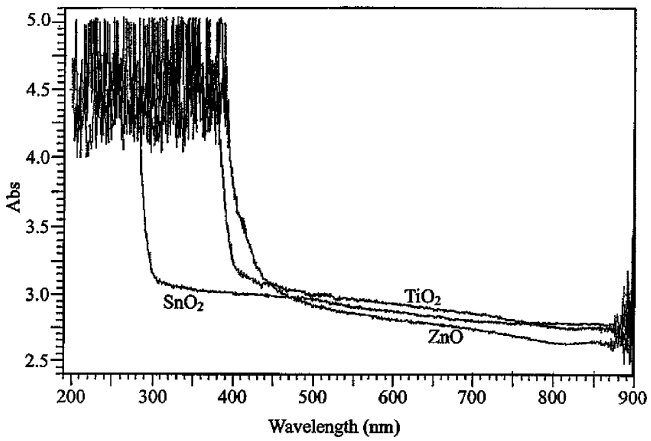

Fig. 3. The UV–vis spectrum of TiO_2, ZnO and SnO_2.

at half maximum value of the photocatalyst; and θ is the diffraction angle [19]. The diameters of the TiO_2, ZnO and SnO_2 powders were thus calculated to be 24, 27, and 59 nm, respectively. The specific surface areas of TiO_2, ZnO and SnO_2 powders were calculated to be 54.2, 4.6 and 4.8 m^2/g. Fig. 3 showed the UV–vis spectrum of TiO_2, ZnO and SnO_2 particles. The figures reveal that TiO_2 absorbs UV light at wavelengths below 390 nm, ZnO absorbs light at wavelengths below 430 nm and SnO_2 absorbs UV light at wavelengths below 290 nm. Substituting the critical wavelengths of TiO_2 = 391 nm, ZnO = 425 nm and SnO_2 = 300 nm into the Planck equation ($E = h\nu$), the band gap energies of TiO_2, ZnO and SnO_2 are 3.17, 2.92 and 4.13 eV, respectively. For comparison, the band gap energies of TiO_2, ZnO and SnO_2 powders determined by other investigators varied from 3.1 to 3.2 eV for TiO_2 [20,21], 3.0–3.2 eV for ZnO [21,22], and 3.5–3.9 eV for SnO_2 [20,23].

TiO_2 has smaller size and, therefore exhibits a much larger specific surface area than ZnO and SnO_2. The corresponding absorption thresholds of TiO_2, ZnO and SnO_2 were 391, 425 and 300 nm, respectively. The light source used had wavelengths between 300 and 450 nm, and the main wavelength was approximately 365 nm (Fig. 4a); hence, the smaller quantum efficiency of SnO_2 with wider band gap due to poor utilization of the UV light was expected. Based on the power distribution of the lamp (Fig. 4b) and the corresponding absorption thresholds of TiO_2 and ZnO, the quantum yield of ZnO might exceed that of TiO_2. However, the photodegradation efficiency was not only affected by the quantum yield of photocatalyst but was also influenced by the specific surface area and size of the particles.

3.2. Photodegradation of 1,2,3,6,7,8-HxCDD and OCDD

The analytical methods were validated by determining recovery efficiencies. US EPA method 1613 [18] requires samples to be reanalyzed if the recovery efficiency of the [^{13}C]-labeled internal standards falls outside the range 30–140%.

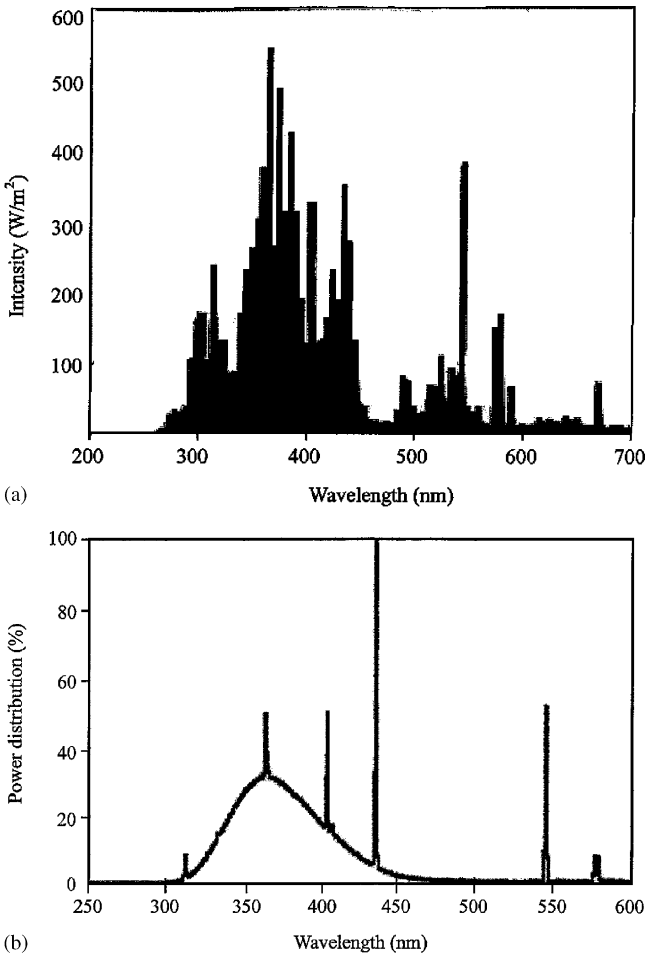

Fig. 4. The spectra of light source (a) emission spectrum (b) power distribution.

The recovery efficiencies obtained by the 1,2,3,6,7,8-HxCDD and OCDD analyze ranged from 75% to 140%, implying the acceptability of the analytical procedures (Tables 1 and 2). Consequently, the results of 1,2,3,6,7,8-HxCDD and OCDD

Table 1
Detection limits and recovery efficiencies of the PCDD/Fs in the HxCDD analytical procedures (n = 9)

PCDD/Fs	Detection limit (pg)	Recovery (%)
2,3,7,8-TeCDF	0.28 ± 0.15	112 ± 7
1,2,3,7,8-PeCDF	0.58 ± 0.24	136 ± 6
2,3,4,7,8-PeCDF	0.61 ± 0.26	115 ± 9
1,2,3,4,7,8-HxCDF	1.03 ± 0.43	93 ± 2
1,2,3,6,7,8-HxCDF	0.96 ± 0.40	92 ± 3
2,3,4,6,7,8-HxCDF	0.98 ± 0.41	91 ± 3
1,2,3,7,8,9-HxCDF	1.15 ± 0.48	85 ± 3
1,2,3,4,6,7,8-HpCDF	0.81 ± 0.28	92 ± 3
1,2,3,4,7,8,9-HpCDF	0.97 ± 0.33	81 ± 6
2,3,7,8-TeCDD	0.58 ± 0.37	99 ± 6
1,2,3,7,8-PeCDD	0.49 ± 0.17	108 ± 8
1,2,3,4,7,8-HxCDD	0.72 ± 0.31	90 ± 2
1,2,3,6,7,8-HxCDD	0.68 ± 0.29	100 ± 4
1,2,3,4,6,7,8-HpCDD	1.05 ± 0.50	93 ± 3
OCDD	0.70 ± 0.25	87 ± 5

Table 2
Detection limits and recovery efficiencies of the PCDD/Fs in the OCDD analytical procedures (n = 9)

PCDD/Fs	Detection limit (pg)	Recovery (%)
2,3,7,8-TeCDF	0.38 ± 0.16	91 ± 10
1,2,3,7,8-PeCDF	0.97 ± 0.41	105 ± 15
2,3,4,7,8-PeCDF	1.01 ± 0.43	99 ± 15
1,2,3,4,7,8-HxCDF	1.44 ± 0.39	78 ± 4
1,2,3,6,7,8-HxCDF	1.34 ± 0.36	79 ± 4
2,3,4,6,7,8-HxCDF	1.36 ± 0.37	78 ± 4
1,2,3,7,8,9-HxCDF	1.61 ± 0.43	77 ± 3
1,2,3,4,6,7,8-HpCDF	1.30 ± 0.38	82 ± 5
1,2,3,4,7,8,9-HpCDF	1.55 ± 0.45	84 ± 5
2,3,7,8-TeCDD	0.82 ± 0.39	94 ± 10
1,2,3,7,8-PeCDD	0.77 ± 0.23	110 ± 14
1,2,3,4,7,8-HxCDD	1.07 ± 0.19	92 ± 3
1,2,3,6,7,8-HxCDD	1.02 ± 0.18	99 ± 6
1,2,3,4,6,7,8-HpCDD	1.46 ± 0.38	97 ± 5
OCDD	1.81 ± 2.01	112 ± 7

quantified with reference to the known concentration of the [^{13}C]-labeled internal standards should be valid.

Fig. 5 plots photodegradation of 1,2,3,6,7,8-HxCDD and OCDD using immobilized TiO_2, ZnO and SnO_2. The reaction rates are found to follow the first-order as was also reported by others for photodegradation of dioxins [9–12]. The reaction of 1,2,3,6,7,8-HxCDD in the UV/TiO_2 system proceeds too fast to determine the corresponding first-order rate constants (Fig. 5a). Table 3 compares the reaction rate constants for PCDDs determined from the present study with those of others. In general, the photodegradation of 1,2,3,6,7,8-HxCDD is faster than that of OCDD, suggesting that the chlorine substitution pattern on the dibenzo-*p*-dioxin affects the selectivity of photocatalytic reactions. In particular, photodegradation rates declined as the number of chloro-substituent increased, implying that higher chlorinated PCDD/Fs are less susceptible to photodegradation. This may partially due to the fact that with a large number of chlorines on PCDDs, the electron density on the aromatic ring decreased resulting in the decreased rate of electrophilic OH addition [11]. Similar findings of the difficulty to degrade more chlorine-substituted dioxins were also reported by others [9–11]. The first-order reaction rate constant of OCDD by UV/TiO_2 in this study was approximately one-order of magnitude higher than that of Choi et al. [11] who used a similar TiO_2 film. It is unclear as to the reason for the observed fast rate in our study; their slower rate perhaps is due to the use of much higher dioxin concentration (6200 ng/cm^2 versus our 12.5 ng/cm^2) which may result in potential product inhibition.

In the photolysis of HxCDD, the k value of sunlight in general is smaller than that of UV (Table 3). The use of catalysts, in particular in the immobilized phase, provides one to two orders of magnitude higher reaction rates than the

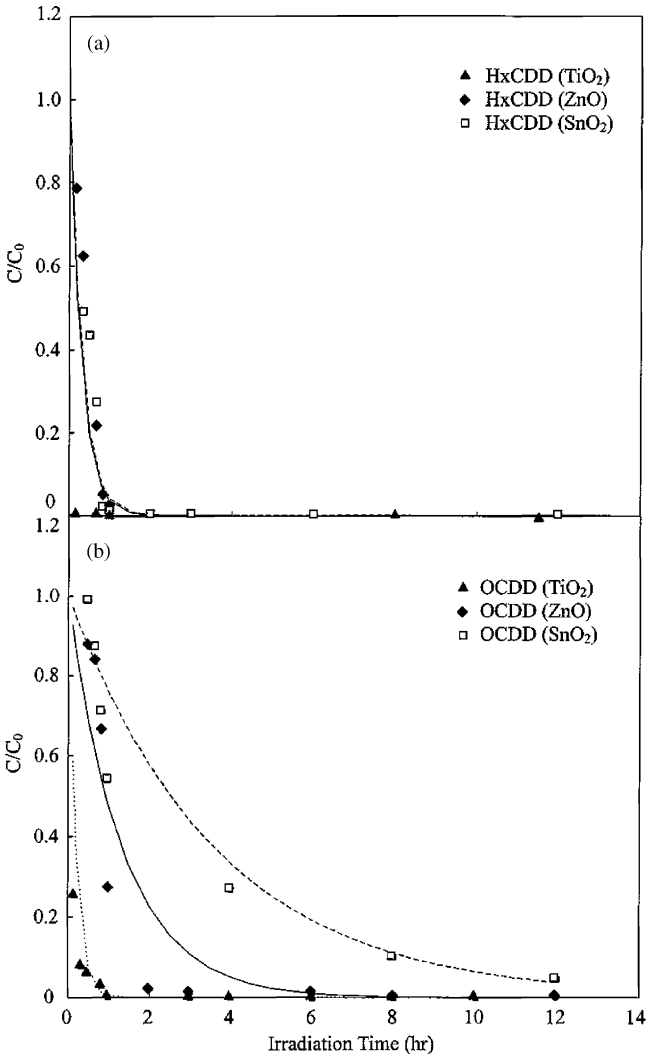

Fig. 5. Photodegradation of PCDDs by different photocatalysts at the initial PCDDs dosage = 50 ng (a) 1,2,3,6,7,8-HxCDD, (b) OCDD. The light intensity = 6.33 mW/cm^2. The lines represent the first-order predicted values.

Table 3
Summary of the first-order reaction rate constants (k) of OCDD and HxCDD

	k (h^{-1})	Reference
OCDD		
UV (pure water)	0.01	[9]
UV (60% acetonitrile/water)	0.06	[9]
UV	0.17	[24]
UV	0.01	[25]
UV	1.00	[12]
Sunlight	<0.01	[10]
Sunlight	0.16	[24]
O_3	0.37	[12]
UV/O_3	1.09	[12]
UV/H_2O_2	0.04	[25]
UV/TiO_2	0.12	[11]
UV/TiO_2	5.30	This study
UV/ZnO	0.74	This study
UV/SnO_2	0.28	This study
HxCDD		
UV/1,2,3,6,7,8-HxCDD	0.06	[26]
Sunlight/1,2,3,6,7,8-HxCDD	0.01	[10]
UV/TiO_2/1,2,3,6,7,8-HxCDD	Very fast	This study
UV/ZnO/1,2,3,6,7,8-HxCDD	3.28	This study
UV/SnO_2/1,2,3,6,7,8-HxCDD	3.19	This study

photolysis alone. The photocatalytic reaction rate of OCDD, as would be expected, exceeds that of the simple photolysis reaction. Table 3 further indicates that the reaction rate constants follow the order: UV/TiO_2 > UV/ZnO > UV/SnO_2 > UV > sunlight. For HxCDD, the rate is similar for both ZnO and SnO_2 due to its easy degradation as compared to OCDD. With almost the same specific surface area (4.6–4.8 m^2/g), the photocatalytic degradation of OCDD using ZnO is faster than that with SnO_2. The absorption threshold of photocatalysts might be responsible for the observed higher rate in ZnO. The corresponding adsorption threshold of ZnO and SnO_2 are 425 and 300 nm, respectively, suggesting that ZnO absorbs a large fraction of UV, and hence more photons than SnO_2 from the same light source used (Fig. 4). Accordingly, the rate of photoexcitation of ZnO is higher than that of SnO_2, perhaps resulting from more OH radicals, excited holes and electrons. Sakthivel et al. [21] also stated that the photocatalytic activity with the Acid Brown 14 dye also followed the order ZnO > SnO_2, due to the fact that light energy could not excite SnO_2 with a wide band gap.

The rate constant of the reaction of OCDD obtained with UV/TiO_2 exceeded that obtained with UV/ZnO by approximately one order of magnitude (Table 3). Since TiO_2 and ZnO could be photoexcited under the light source used in this study, the higher photocatalytic activity of TiO_2 may be due to its larger specific surface area. On the contrary, numerous studies have demonstrated that ZnO is a more powerful photocatalyst than TiO_2 for photodegrading a variety of organics [21,27,28]. However, all these studies involved in the photodegradation of organics in solution with the suspended ZnO particles. Hence, the extent of photocatalytic activity obtained from other studies may differ from that in the immobilized phase used in the present study.

Care must be taken to control the generation of byproducts which may be more toxic than the parent pollutants, if mineralization is not complete. For the present study, all 2,3,7,8-substituted congeners were not detected, perhaps due to the following reasons: (i) the photocatalytic degradation involved the cleavage of the aromatic ring, as noted by Choi et al. [11], and/or (ii) the removal of lateral chlorines was favored over the removal of longitudinal ones from OCDD. Although photodegradation of OCDD in the solution phase involves preferential chlorine loss at lateral positions (2,3,7,8) over loss at longitudinal positions (1,4,6,9) [12,29,30], as with HxCDD [8], congeners with longitudinal chlorines degrade more rapidly than those with laterally substituted chlorines in the surface-phase reaction [31]. Thus, the speculation of the degradation of OCDD and HxCDD in the present study is that the cleavage of the aromatic ring may dominate the reaction pathway. Unfortunately, due to the low dosage (50 ng) of target compounds used, the amounts of Cl^- and total organic carbon were too small for quantification. Nonetheless, the UV/photocatalyst system may offer an effective treatment for PCDDs as far as no detection of 2,3,7,8-substituted congeners was concerned.

4. Conclusions

XRD results revealed that sintered photocatalysts at 400 °C did not affect their properties. The structure of TiO_2 includes both anatase and rutile phases, and that ZnO and SnO_2 with a typical zincite and cassiterite phase, respectively. The mean particle sizes followed the order SnO_2 > ZnO > TiO_2; TiO_2 had the largest specific surface area of these photocatalysts. The photoactivities of TiO_2, ZnO and SnO_2 for 1,2,3,6,7,8-HxCDD and OCDD using immobilized photocatalyst films were compared. The photodegradation of 1,2,3,6,7,8-HxCDD is faster than that of OCDD, suggesting that the chlorine substitution pattern influences the selectivity of photocatalytic reactions. Photodegradation rates decline as the number of chlorine atoms increases. The first-order reaction rate constants follow the order of UV/TiO_2 > UV/ZnO > UV/SnO_2 > UV. TiO_2 and ZnO are believed to absorb a large fraction of UV, and probably absorbed more photons than SnO_2 from the light source used. Congeners with longitudinal chlorines degrade more rapidly than those with laterally substituted chlorines from PCDDs in surface-phase reaction, and no 2,3,7,8-substituted congeners was detected, therefore, this work suggests that the cleavage of the aromatic ring may dominate the reaction pathway in UV/photocatalyst systems.

Acknowledgements

The authors would like to thank the National Science Council of the Republic of China for financially supporting this research under Contract No. NSC 92-2621-Z-264-001.

References

[1] M.S. McLachlan, A.P. Sewart, J.R. Bacon, K.C. Jones, Persistence of PCDD/Fs in a sludge amended soil, Environ. Sci. Technol. 30 (1996) 2567–2571.
[2] H.J. Geyer, K.W. Schramm, E.A. Feicht, A. Behechti, C. Steinberg, R. Bruggemann, H. Poiger, B. Henkelmann, A. Kettrup, Half-lives of tetra-, penta-, hexa-, hepta-, and octachlorodibenzo-*p*-dioxin in rats, monkeys, and humans – a critical review, Chemosphere 48 (2002) 631–644.
[3] P.S. Cheng, M.S. Hsu, E. Ma, U. Chou, Y.C. Ling, Levels of PCDD/Fs in ambient air and soil in the vicinity of a municipal solid waste incinerator in Hsinchu, Chemosphere 52 (2003) 1389–1396.
[4] S.C. Kim, S.H. Jeon, I.R. Jung, K.H. Kim, M.H. Kwon, J.H. Kim, J.H. Yi, S.J. Kim, J.C. You, D.H. Jung, Formation and emission status of PCDDs/PCDFs in municipal solid waste incinerators in Korea, Chemosphere 43 (2001) 701–707.
[5] H.W. Ma, Y.L. Lai, C.C. Chan, Transfer of dioxin risk between nine major municipal waste incinerators in Taiwan, Environ. Int. 28 (2002) 103–110.
[6] G. McKay, Dioxin characterization, formation and minimization during municipal solid waste (MSW) incineration: review, Chem. Eng. J. 86 (2002) 343–368.
[7] R. Lohmann, K.C. Jones, Dioxins and furans in air and deposition: a review of levels, behavious and processes, Sci. Total Environ. 219 (1998) 53–81.

[8] N. Kluyev, A. Cheleptchikov, E. Brodsky, V. Soyfer, V. Zhilnikov, Reductive dechlorination of polychlorinated dibenzo-*p*-dioxins by zerovalent iron in subcritical water, Chemosphere 46 (2002) 1293–1296.
[9] M. Kim, P.W. O'Keefe, Photodegradation of polychlorinated dibenzo-*p*-dioxins and dibenzofurans in aqueous solutions and in organic solvents, Chemosphere 41 (2000) 793–800.
[10] J. Niu, J. Chen, B. Henkelmann, X. Quan, F. Yang, A. Kettrup, K.W. Schramm, Photodegradation of PCDD/Fs adsorbed on spruce (*Picea abies* (L.) Karst.) needles under sunlight irradiation, Chemosphere 50 (2003) 1217–1225.
[11] W. Choi, S.J. Hong, Y.S. Chang, Y. Cho, Photocatalytic degradation of polychlorinated dibenzo-*p*-dioxins on TiO_2 film under UV or solar light irradiation, Environ. Sci. Technol. 34 (2000) 4810–4815.
[12] H. Minami, Y. Terao, Y. Horii, T. Nakao, H. Miyata, UV/ozone/nitrogen/hydrogen-photolysis of dioxins in water, Organohalogen Comp. 45 (2000) 360–363.
[13] H. Muto, K. Saitoh, H. Funayama, PCDD/DF formations by the heterogeneous thermal reactions of phenols and their TiO_2 photocatalytic degradation by batch-recycle system, Chemosphere 45 (2001) 129–136.
[14] Y.S. Choi, B.W. Kim, Photocatalytic disinfection of *E. coli*. In a UV/TiO_2-immobilised optical-fiber reactor, J. Chem. Technol. Biotechnol. 75 (2000) 1145–1150.
[15] M.B. Chang, Y.M. Weng, T.Y. Lee, Y.W. Chen, S.H. Chang, K.H. Chi, Sampling and analysis of ambient dioxins in northern Taiwan, Chemosphere 51 (2003) 1103–1110.
[16] A. Fernandez, G. Lassaletta, V.M. Jimenez, A. Justo, A.R. Gonzalez-Elipe, J.M. Herrmann, H. Tahiri, Y. Ait-Ichou, Preparation and characterization of TiO_2 photocatalysts supported on various rigid supports (glass, quartz and stainless steel), Appl. Catal. B: Environ. 7 (1995) 49–63.
[17] B. Pal, M. Sharon, Photodegradation of polyaromatic hydrocarbons over thin film of TiO_2 nanoparticles; a study of intermediate photoproducts, J. Mol. Catal. A: Chem. 160 (2000) 453–460.
[18] U.S. Environmental Protection Agency, Method-1613: tetra-through octa chlorinated dioxins and furans by isotope dilution HRGC/HRMS, Revision B, 1995.
[19] H.P. Klug, L.E. Alexander, X-ray Diffraction Procedures for Polycrystalline and Amorphous Materials, Wiley/Interscience, New York, 1974.
[20] K. Vinodgopal, P.V. Kamat, Enhanced rates of photocatalytic degradation of an azo dye using SnO_2/TiO_2 coupled semiconductor thin films, Environ. Sci. Technol. 29 (1995) 841–845.
[21] S. Sakthivel, B. Neppolian, M.V. Shankar, B. Arabindoo, M. Palanichamy, V. Murugesan, Solar photocatalytic degradation of azo dye: comparison of photocatalytic efficiency of ZnO and TiO_2, Solar Energy Mater. Solar Cells 77 (2003) 65–82.
[22] N. Serpone, P. Maruthamuthu, P. Pichat, E. Pelizzetti, H. Hidaka, Exploiting the interparticle electron transfer process in the photocatalysed oxidation of phenol, 2-chlorophenol and pentachlorophenol: chemical evidence for electron and hole transfer between coupled semiconductors, J. Photochem. Photobiol. A: Chem. 85 (1995) 247–255.
[23] J.C. Bernede, S. Marsillac, Band alignment at the interface of a SnO_2/γ-In_2Se_3 heterojunction, Mater. Res. Bull. 32 (1997) 1193–1200.
[24] F. Schuler, P. Schmid, C. Schlatter, Photodegradation of polychlorinated dibenzo-*p*-dioxins and dibenzofurans in cuticular waxes of laurel cherry (*Prunus laurocerasus*), Chemosphere 36 (1998) 21–34.
[25] Q. Yan, S. Kapila, L.D. Sivils, A.A. Elseewi, Effects of sensitizers and inhibitors on phototransformation of polychlorinated dibenzo-*p*-dioxins (PCDDs), Chemosphere 31 (1995) 3627–3634.
[26] C.H. Wu, G.P. Chang-Chien, W.S. Lee, Photolytic methods for degradation of polychlorinated dibenzo-*p*-dioxins, J. Hazard. Mater. (2004).
[27] C.A.K. Gouvea, F. Wypych, S.G. Moraes, N. Duran, N. Nagata, P. Peralta-Zamora, Semiconductor-assisted photocatalytic degradation of reactive dyes in aqueous solution, Chemosphere 40 (2000) 433–440.
[28] A.A. Khodja, T. Sehili, J.F. Pilichowski, P. Boule, Photocatalytic degradation of 2-phenylphenol on TiO_2 and ZnO in aqueous suspensions, J. Photochem. Photobiol. A: Chem. 141 (2001) 231–239.
[29] M.M. Lynam, M. Kuty, J. Damborsky, J. Koca, P. Adriaens, Molecular orbital calculations to describe microbial reductive dechlorination of polychlorinated dioxins, Environ. Toxicol. Chem. 17 (1998) 988–997.
[30] H. Fueno, K. Tanaka, S. Sugawa, Theoretical study of the dechlorination reaction pathways of octachlorodibenzo-*p*-dioxin, Chemosphere 48 (2002) 771–778.
[31] M.H. Schoonenboom, H.E. Zoetemeijer, K. Olie, Dechlorination of octachlordibenzo-*p*-dioxin and octachlorodibenzofuran on alumina support, Appl. Catal. B: Environ. 6 (1995) 11–20.